CARRIER DYNAMICS OF ABNORMAL TEMPERATURE-DEPENDENT EMISSION SHIFT IN MOCVD-GROWN InGaN EPILAYERS AND InGaN/GaN QUANTUM WELLS

Yong-Hoon Cho*, B. D. Little*, G. H. Gainer*, J. J. Song*,
S. Keller**, U. K. Mishra**, and S. P. DenBaars**

*Center for Laser and Photonics Research and Department of Physics
Oklahoma State University, Stillwater, OK 74078
**Electrical and Computer Engineering and Materials Departments
University of California, Santa Barbara, CA 93106

Cite this article as: MRS Internet J. Nitride Semicond. Res. 4S1, G2.4 (1999)

ABSTRACT

Temperature-dependent photoluminescence (PL) studies have been performed on InGaN epilayers and InGaN/GaN multiple quantum wells (MQWs) grown by metalorganic chemical vapor deposition. We observed anomalous temperature dependent emission behavior (specifically an S-shaped decrease-increase-decrease) of the peak energy (E_{PL}) of the InGaN-related PL emission with increasing temperature. In the case of the InGaN epilayer, E_{PL} decreases in the temperature range of 10 – 50 K, increases for 50 – 110 K, and decreases again for 110 – 300 K with increasing temperature. For the InGaN/GaN MQWs, E_{PL} decreases from 10 – 70 K, increases from 70 – 150 K, then decreases again for 150 – 300 K. The actual temperature dependence of the PL emission was estimated with respect to the bandgap energy determined by photoreflectance spectra. We observed that the PL peak emission shift has an excellent correlation with a change in carrier lifetime with temperature. We demonstrate that the temperature-induced S-shaped PL shift is caused by the change in carrier recombination dynamics with increasing temperature due to inhomogeneities in the InGaN structures.

INTRODUCTION

In spite of the recent rapid achievements in the area of InGaN-based light emitting devices, the fundamental mechanisms of spontaneous and stimulated emission are still in debate in these materials. Recently, it has been pointed out that strain-induced piezoelectric fields in InGaN/GaN quantum wells (QWs) may play an important role in the spontaneous recombination process [1,2]. On the other hand, recombination from localized band-tail states at potential fluctuations or even from quantum-dot-like deep traps originating from In-rich regions in the wells has also been proposed as a principal spontaneous emission mechanism in InGaN/GaN QWs [3-11]. The main difficulty in distinguishing between these two effects partly originates from the fact that both effects can explain - at least qualitatively - some experimental observations such as a large Stokes shift of the luminescence and an emission redshifting behavior with time [1-9]. More recently, a temperature-induced luminescence blueshift was observed in InGaN single QWs [10,11] and multiple QWs (MQWs) [6], which has been well explained by an involvement of band-tail states but can hardly be explained by the piezoelectric field effect alone. Therefore, a detailed understanding of the carrier dynamics and its relationship to the emission mechanism as a function of temperature are very important for both InGaN epilayers and InGaN/GaN MQWs.

In this study, we report a systematic photoluminescence (PL) study of InGaN epilayers and InGaN/GaN MQWs as a function of temperature by means of PL, PL excitation (PLE), and time-resolved PL (TRPL) spectroscopy. As the temperature is increased, the peak energy position of the InGaN-related PL emission (E_{PL}) exhibits an S-shaped behavior (redshift-blueshift-redshift). In the case of the InGaN epilayer, E_{PL} decreases in the temperature range of 10 – 50 K, increases for 50 – 110 K, and decreases again for 110 – 300 K with increasing temperature. For the InGaN/GaN MQWs, E_{PL} decreases from 10 – 70 K, increases from 70 – 150 K, then decreases again from 150 – 300 K. This temperature-induced S-shaped PL shift is strongly affected by the change in carrier dynamics with increasing temperature for both the InGaN epilayer and the InGaN/GaN MQWs.

EXPERIMENT

The InGaN epilayers and the InGaN/GaN MQWs used in this study were grown on c-plane sapphire films by metalorganic chemical vapor deposition (MOCVD), following the deposition of a 1.8-μm-thick GaN buffer layer. For the InGaN epilayers, a 100-nm-thick InGaN layer was capped with a 50-nm-thick GaN layer. The MQW structures consisted of 12 MQWs with 3-nm-thick InGaN wells and 4.5-nm-thick GaN barriers, with a 100-nm-thick $Al_{0.07}Ga_{0.93}N$ capping layer. The growth temperatures of the GaN base layer, the MQW regions, and the AlGaN capping layer were 1050, 790, and 1040 ^{o}C, respectively. The In content of the InGaN layers was estimated to be about 18 % for both the epilayer and the MQWs by means of high-resolution x-ray diffraction measurements. We observed optically pumped stimulated emission from the MQW sample with a low threshold density (< 60 kW/cm^2) at room temperature. Details of the growth procedure and results of other structural and optical properties were reported elsewhere [12-15]. Additionally, the influence of Si doping in the GaN barriers of the MQWs on the optical properties is also given elsewhere [7]. PL spectra were measured as a function of temperature ranging from 10 to 300 K using the 325 nm line of a 20 mW cw He-Cd laser. PLE spectra were measured using the quasi-monochromatic light from a xenon lamp dispersed by a 1/2 m monochromator. TRPL measurements were carried out using a picosecond pulsed laser system consisting of a cavity-dumped dye laser synchronously pumped by a frequency-doubled modelocked Nd:YAG laser for sample excitation and a streak camera for detection. The overall time resolution of the system is better than 15 ps.

RESULTS AND DISCUSSIONS

Figure 1 shows 10 K PL and PLE spectra of the InGaN-related emission with a peak energy of ~ 2.99 and ~ 2.76 eV for (a) the InGaN epilayer and (b) the InGaN/GaN MQWs, respectively. A large Stokes shift of the InGaN emission between the PL peak energy and the band-edge obtained from the PLE spectra is clearly observed, which is mainly due to crystal imperfections such as In alloy fluctuations and/or interface roughness. We note that the observed Stokes shift for the MQWs is much larger than that of the epilayer, probably due to the influence of the MQW interfaces on the overall potential fluctuations. In general, the fundamental temperature-induced energy gap shrinkage of GaN, InGaN, and AlGaN can be described by the Varshni empirical equation [16]: $E_g(T) = E_g(0) - a\,T^{2}/(b + T)$, where $E_g(T)$ is the bandgap transition energy at a temperature T, and a and b are known as the Varshni thermal coefficients. Previously, from photoreflectance studies, the parameters a = 8.32 (10) x 10^{-4} eV/K and b = 835.6 (1196) K for the GaN G_9^V - G_7^C ($In_{0.14}Ga_{0.86}N$) transition were obtained [17]. For simplicity, Varshni thermal coefficients obtained from the GaN and $In_{0.14}Ga_{0.86}N$ transitions [17] were used for the E_g estimation of the $Al_{0.07}Ga_{0.93}N$ and $In_{0.18}Ga_{0.82}N$ layers, respectively. The temperature-dependent PL peak shift for the GaN and AlGaN layers was consistent with the estimated energy decrease of about 65 meV between 10 and 300 K, whereas the InGaN-related

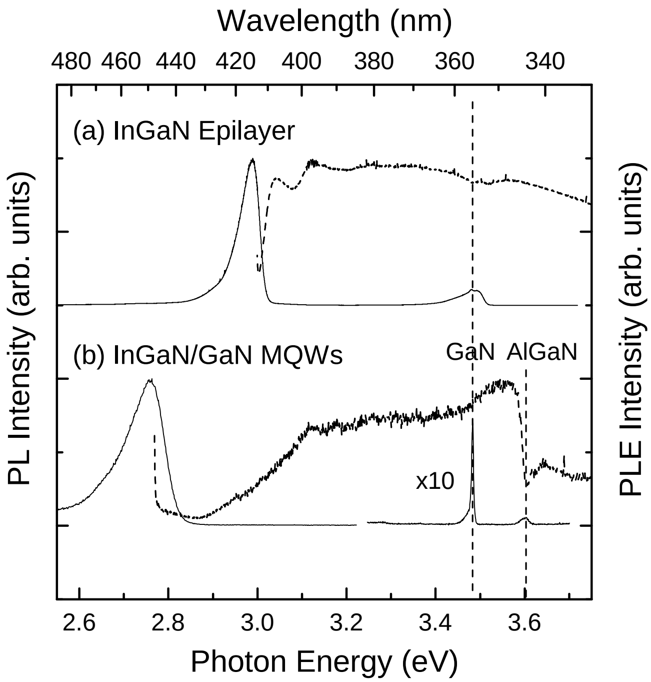

Figure 1. 10 K PL (solid lines) and PLE (dashed lines) spectra of (a) the InGaN epilayer and (b) the InGaN/GaN MQWs. A large Stokes shift of the PL emission from the InGaN layers with respect to the band-edge measured by PLE spectra is observed. Near-band-edge emission from the GaN and AlGaN layers was observed at 3.48 and 3.6 eV, respectively. The PLE contributions from the GaN layers [in (a) and (b)] and the AlGaN layer [in (b)] are clearly seen.

PL emission did not follow the typical temperature dependence of the energy gap shrinkage as will be shown later.

Figure 2 shows the evolution of the InGaN-related PL spectra for (a) the InGaN epilayer and (b) the InGaN/GaN MQWs over a temperature range from 10 to 300 K. As the temperature increases from 10 K to T_I, where T_I is 50 (70) K for the epilayer (MQWs), E_{PL} redshifts 10 (19) meV. This value is about five times larger than the expected bandgap shrinkage of ~ 2 (4) meV for the epilayer (MQWs) over this temperature range [17]. For a further increase in temperature, the PL peak blueshifts 22.5 (14) meV from T_I to T_{II}, where T_{II} is 110 (150) K for the epilayer (MQWs). By considering the estimated temperature-induced bandgap shrinkage of ~ 7 (13) meV for the epilayer (MQWs), the actual blueshift of the PL peak with respect to the band-edge is about 29.5 (27) meV over this temperature range. When the temperature is further increased above T_{II}, the peak positions redshift again. From the observed redshift of 45 (16) meV and the expected bandgap shrinkage of ~ 51 (43) meV from T_{II} to 300 K for the epilayer (MQWs), we estimate an actual blueshift of the PL peak relative to the band-edge to be about 6 (27) meV in this temperature range.

To elucidate the kinetics of carrier recombination, we performed TRPL measurements over the same temperature range. Figure 3 shows E_{PL}, the relative energy difference (DE) between E_{PL} and E_g at each temperature, and the decay times (t_d) monitored at the peak energy, lower energy side, and higher energy side of the peak as a function of temperature. A comparison of these values clearly shows that the temperature dependence of DE and E_{PL} is strongly correlated with the change in t_d. In both cases, we found an overall increase of t_d with increasing temperature for $T < T_I$, in qualitative agreement with the temperature dependence of radiative recombination [18,19]. Moreover, in this temperature range, t_d becomes longer with decreasing emission energy, and hence, the peak energy of the emission shifts to the low energy side as time proceeds. This behavior is a characteristic of localized carriers, which in this case is most likely related to alloy fluctuations (and/or interface roughness in the MQWs) [7,9]. We note that the observed longer lifetime for the MQWs compared to those reported by other groups is probably due to relatively larger degree of carrier localization caused by a larger number of QWs and/or

https://doi.org/10.1557/S1092578300002271 Published online by Cambridge University Press

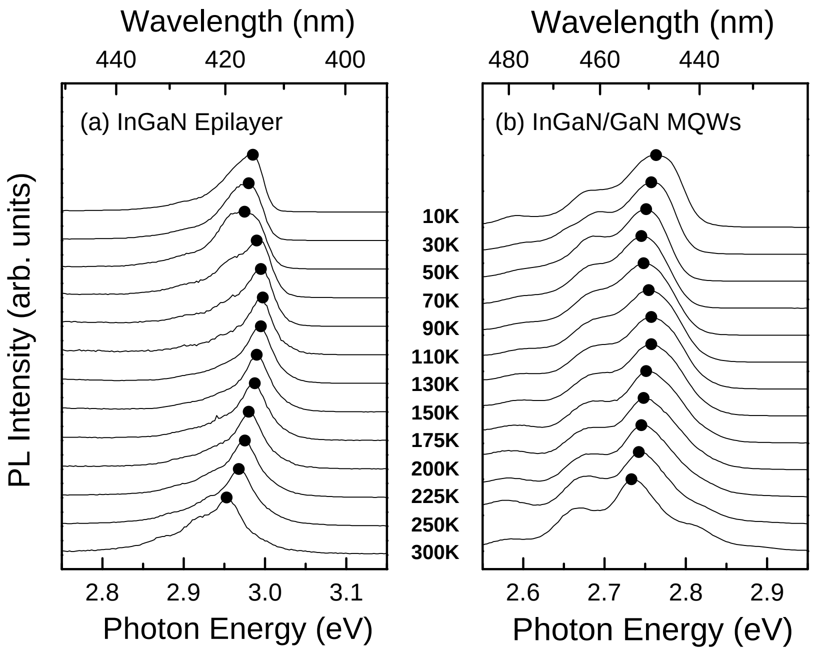

Figure 2. Typical InGaN-related PL spectra for (a) the InGaN epilayer and (b) the InGaN/GaN MQWs in the temperature range from 10 to 300 K. The main emission peak of both samples (closed circles) shows an S-shaped shift with increasing temperature. All spectra are normalized and shifted in the vertical direction for clarity. Note that the turnover temperature from redshift to blueshift occurs at about 50 and 70 K for the InGaN epilayer and the InGaN/GaN MQWs, respectively.

different growth conditions used in this work [3,7,20-22]. As the temperature is further increased beyond T_I, the lifetime of the epilayer (MQWs) quickly decreases to less than 0.1 (10) ns and remains almost constant between T_{II} and 300 K, indicating that non-radiative processes predominantly affect the emission in this range. This is further evidenced by the fact that there is no difference between the lifetimes monitored above, below, and at the peak energy for $T > T_I$, in contrast to the observations for $T < T_I$. This characteristic temperature T_I is also where the turnover occurs from redshift to blueshift for *DE* and E_{PL} with increasing temperature. Furthermore, in the temperature range between T_I and T_{II}, where a blueshift of E_{PL} is detected, t_d dramatically decreases from 0.4 to 0.05 (35 to 8) ns for the epilayer (MQWs). Above T_{II}, where a redshift of E_{PL} is observed, no sudden change in t_d occurs for either the epilayer or the MQWs.

From these results, the InGaN-related recombination mechanism for different temperature ranges can be explained as follows: (i) For $T < T_I$, since the radiative recombination process is dominant, the carrier lifetime increases, giving the carriers more opportunity to relax down into lower energy tail states caused by the inhomogeneous potential fluctuations before recombining. This behavior reduces the higher energy side emission intensity, and thus, produces a redshift in the peak energy position with increasing temperature. (ii) For $T_I < T < T_{II}$, since the dissociation rate is increased and other non-radiative processes become dominant, the carrier lifetime decreases greatly with increasing temperature and also becomes independent of the emission energies. Thus, due to the decreasing lifetime, these carriers recombine before reaching the lower energy tail states. This behavior gives rise to an apparent broadening of the higher energy side emission and leads to a blueshift in the peak energy. (iii) For $T > T_{II}$, since non-radiative recombination processes are dominant and the lifetimes are almost constant [in contrast to the case (ii)], the photogenerated carriers are less affected by the change in carrier lifetime so that the blueshift behavior becomes smaller. Note that the slope of *DE* is very sensitive to the change

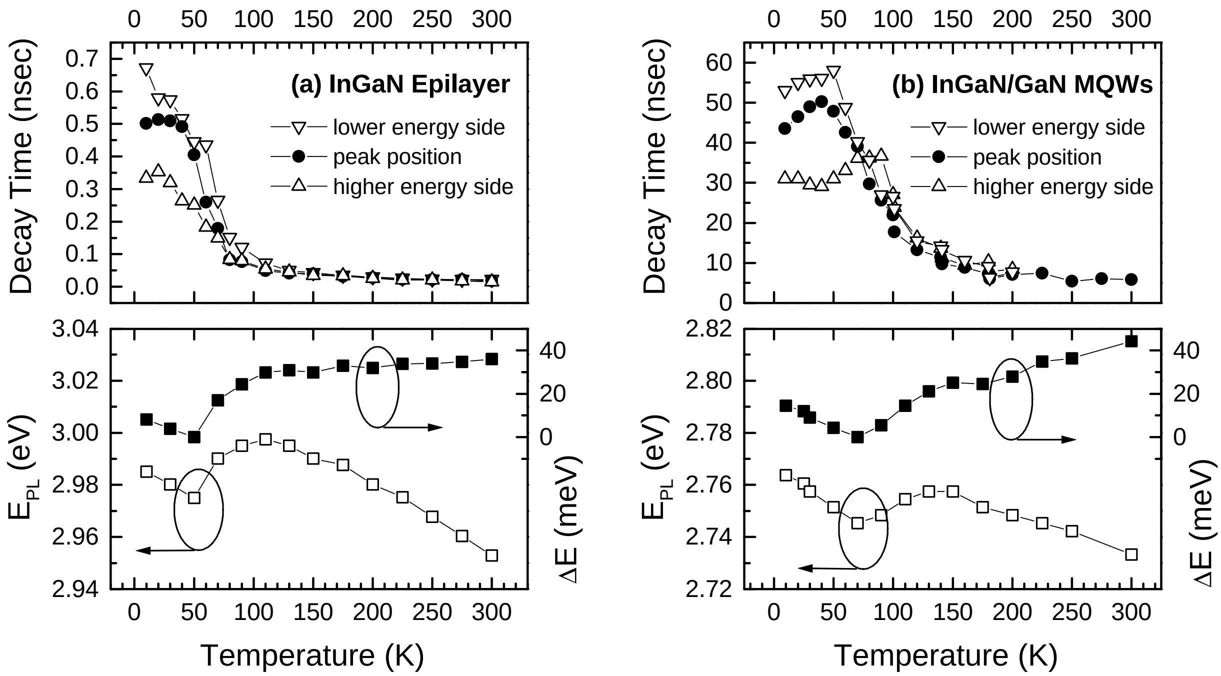

Figure **3.** InGaN-related PL spectral peak position E_{PL} (open squares) and decay time t_d as a function of temperature in (a) the InGaN epilayer and (b) the InGaN/GaN MQWs. *DE* (closed squares) represents the relative energy difference between E_{PL} and E_g at each temperature. The minimum value of *DE* is designated as zero for simplicity. Note that the lower energy side of the PL peak has a longer lifetime than the higher energy side below a certain temperature T_I, while there is no difference between lifetimes monitored above, below, and at the peak energy above T_I,, where T_I is about 50 (70) K for the epilayer (MQWs). This characteristic temperature T_I is also where the turnover occurs from redshift to blueshift of the InGaN PL peak energy with increasing temperature.

in t_d with temperature for both the InGaN epilayer and the InGaN/GaN MQWs. Since this blueshift behavior is smaller than the temperature-induced bandgap shrinkage in this temperature range, the peak position exhibits an overall redshift behavior. Consequently, the change in carrier recombination mechanism with increasing temperature causes the S-shaped redshift-blueshift-redshift behavior of the peak energy for the main InGaN-related emission. Therefore, the InGaN-related spontaneous emission features are significantly affected by different carrier recombination dynamics which vary with temperature, because of band-tail states arising from inhomogeneities such as large In alloy fluctuations, layer thickness variations in the MQWs, and/or defects. It should be noted that we observed similar temperature-induced S-shaped emission behavior for both the InGaN epilayers and the InGaN/GaN MQWs, even though t_d of the latter is about two orders of magnitudes longer than that of the former. This strongly reflects the fact that the anomalous temperature-induced emission shift mainly depends on the change in carrier recombination dynamics rather than the absolute value of t_d.

CONCLUSIONS

We have investigated the time-integrated and time-resolved PL properties of MOCVD-grown InGaN epilayers and InGaN/GaN MQWs over the temperature range of 10 to 300 K. The peak energy of the InGaN-related emission, E_{PL}, exhibited an S-shaped (redshift-blueshift-redshift) behavior with increasing temperature. The PL emission peak position and carrier

https://doi.org/10.1557/S1092578300002271 Published online by Cambridge University Press

lifetime as a function of temperature reveal that the InGaN-related emission is strongly affected by the change in carrier recombination dynamics with increasing temperature for both the InGaN epilayers and the InGaN/GaN MQWs. This anomalous temperature-induced emission behavior is attributed to band-tail states due to inhomogeneities in the InGaN-based material.

ACKNOWLEDGMENTS

This work was supported by AFOSR, ARO, ONR, DARPA, and KOSEF.

REFERENCES

1. T. Takeuchi, S. Sota, M. Katsuragawa, M. Komori, H. Takeuchi, H. Amano, and I. Akasaki, Jpn. J. Appl. Phys., Part 2 **36**, L382 (1997).
2. J. S. Im, H. Kollmer, J. Off, A. Sohmer, F. Scholz, and A. Hangleiter, Phys. Rev. B **57**, R9435 (1998); A. Hangleiter, J. S. Im, H. Kollmer, S. Heppel, J. Off, and F. Scholz, MRS Internet J. Nitride Semicond. Res. **3**, 15 (1998).
3. E. S. Jeon, V. Kozlov, Y. -K. Song, A. Vertikov, M. Kuball, A. V. Nurmikko, H. Liu, C. Chen, R. S. Kern, C. P. Kuo, and M. G. Craford, Appl. Phys. Lett. **69**, 4194 (1996).
4. S. Chichibu, T. Azuhata, T. Sota, and S. Nakamura, Appl. Phys. Lett. **69**, 4188 (1996).
5. P. Perlin, V. Iota, B. A. Weinstein, P. Wisniewski, T. Suski, P. G. Eliseev, and M. Osinski, Appl. Phys. Lett. **70**, 2993 (1997).
6. Y. H. Cho, G. H. Gainer, A. J. Fischer, J. J. Song, S. Keller, U. K. Mishra, and S. P. DenBaars, Appl. Phys. Lett. **73**, 1370 (1998).
7. Y. H. Cho, J. J. Song, S. Keller, M. S. Minsky, E. Hu, U. K. Mishra, and S. P. DenBaars, Appl. Phys. Lett. **73**, 1128 (1998); Y. H. Cho, J. J. Song, S. Keller, U. K. Mishra, and S. P. DenBaars, *ibid*. **73**, 3181 (1998).
8. P. Lefebvre, J. Allegre, B. Gil, A. Kavokine, H. Mathieu, W. Kim, A. Salvador, A. Botchkarev, and H. Morkoc, Phys. Rev. B **57**, R9447 (1998).
9. Y. Narukawa, Y. Kawakami, M. Funato, Sz. Fujita, Sg. Fujita, and S. Nakamura, Appl. Phys. Lett. **70**, 981 (1997); Y. Narukawa, Y. Kawakami, Sz. Fujita, Sg. Fujita, and S. Nakamura, Phys. Rev. B **55**, R1938 (1997).
10. P. G. Eliseev, P. Perlin, J. Lee, and M. Osinski, Appl. Phys. Lett. **71**, 569 (1997).
11. K. G. Zolina, V. E. Kudryashov, A. N. Turkin, and A. E. Yunovich, MRS Internet J. Nitride Semicond. Res. **1**, Art, 11 (1996).
12. S. Keller, A. C. Abare, M. S. Minsky, X. H. Wu, M. P. Mack, J. S. Speck, E. Hu, L. A. Coldren, U. K. Mishra, and S. P. DenBaars, Materials Science Forum **264 - 268**, 1157 (1998).
13. S. Bidnyk, T. J. Schmidt, Y. H. Cho, G. H. Gainer, J. J. Song, S. Keller, U. K. Mishra, and S. P. DenBaars, Appl. Phys. Lett. **72**, 1623 (1998).
14. T. J. Schmidt, Y. H. Cho, G. H. Gainer, J. J. Song, S. Keller, U. K. Mishra, and S. P. DenBaars, Appl. Phys. Lett. **73**, 560 (1998); *ibid*. **73**, 1892 (1998).
15. Y. H. Cho, F. Fedler, R. J. Hauenstein, G. H. Park, J. J. Song, S. Keller, U. K. Mishra, and S. P. DenBaars, J. Appl. Phys. (to be published).
16. Y. P. Varshni, Physica **34**, 149 (1967).
17. W. Shan, T. J. Schmidt, X. H. Yang, S. J. Hwang, J. J. Song, and B. Goldenberg, Appl. Phys. Lett. **66**, 985 (1995); W. Shan, B. D. Little, J. J. Song, Z. C. Feng, M. Schurman, and R. A. Stall, *ibid*. **69**, 3315 (1996).
18. B. K. Ridley, Phys. Rev. B **41**, 12 190 (1990).
19. J. Feldmann, G. Peter, E. O. Gobel, P. Dawson, K. Moore, C. Foxon, and R. J. Elliott, Phys. Rev. Lett. **59**, 2337 (1987).
20. C. I. Harris, B. Monemar, H. Amano, and I. Akasaki, Appl. Phys. Lett. **67**, 840 (1995).
21. C. K. Sun, S. Keller, G. Wang, M. S. Minsky, J. E. Bowers, and S. P. DenBaars, Appl. Phys. Lett. **69**, 1936 (1996).
22. J. S. Im, V. Harle, F. Scholz, and A. Hangleiter, MRS Internet J. Nitride Semicond. Res. **1**, 37 (1996).